Cell Reports
Report

Blocking Apoptotic Signaling Rescues Axon Guidance in *Netrin* Mutants

Gunnar Newquist,[1] J. Michelle Drennan,[2] Matthew Lamanuzzi,[1] Kirsti Walker,[1] James C. Clemens,[2] and Thomas Kidd[1,*]
[1]Department of Biology, University of Nevada, Reno, NV 89557, USA
[2]Department of Biochemistry, Purdue University, West Lafayette, IN 47907, USA
*Correspondence: tkidd@unr.edu
http://dx.doi.org/10.1016/j.celrep.2013.02.017

SUMMARY

Netrins are guidance cues that form gradients to guide growing axons. We uncover a mechanism for axon guidance by demonstrating that axons can accurately navigate in the absence of a Netrin gradient if apoptotic signaling is blocked. Deletion of the two *Drosophila NetA* and *NetB* genes leads to guidance defects and increased apoptosis, and expression of either gene at the midline is sufficient to rescue the connectivity defects and cell death. Surprisingly, pan-neuronal expression of *NetB* rescues equally well, even though no Netrin gradient has been established. Furthermore, *NetB* expression blocks apoptosis, suggesting that NetB acts as a neurotrophic factor. In contrast, neuronal expression of *NetA* increases axon defects. Simply blocking apoptosis in *NetAB* mutants is sufficient to rescue connectivity, and inhibition of caspase activity in subsets of neurons rescues guidance independently of survival. In contrast to the traditional role of Netrin as simply a guidance cue, our results demonstrate that guidance and survival activities may be functionally related.

INTRODUCTION

In developing vertebrate nervous systems, a substantial proportion of all neurons born during development die. Neuronal death is frequently due to a failure to successfully compete for a limited supply of survival factors known as neurotrophic factors (reviewed in Oppenheim and von Bartheld, 2008). In *Drosophila*, analysis of eye development has provided strong evidence for the existence of glia-derived molecules providing trophic support for neurons (Buchanan and Benzer, 1993; Xiong and Montell, 1995; Dearborn and Kunes, 2004). These trophic mechanisms are dependent on correct axonal connectivity (Steller et al., 1987; Campos et al., 1992), but the identity of the effector molecules is not yet known (Hidalgo et al., 2011). Earlier in eye development, the epidermal growth factor receptor ligand Spitz acts as a neuronal survival factor that is present in a limited amount (Bergmann et al., 1998, Domínguez et al., 1998; Kurada and White, 1998; Baker and Yu, 2001; Yang and Baker, 2003).

During embryonic development of the fly, apoptosis is widespread and occurs in reproducible patterns (Abrams et al., 1993). Death is particularly obvious in the midline of the ventral nerve cord (VNC; Sonnenfeld and Jacobs, 1995), and epidermal growth factor derived from axons has been shown to be a trophic support factor for the midline glia (MG; Bergmann et al., 2002). Apoptosis in the VNC increases with age, initially in a symmetrical pattern on either side of the midline, suggesting that death is predetermined by developmental lineage. However, a significant proportion of the death is asymmetrical, suggesting that external cues might mediate survival (Abrams et al., 1993; Rogulja-Ortmann et al., 2007). These survival signals are in part derived from non-MG including the longitudinal glia encountered by navigating axons; genetic ablation of the glia leads to increased neuronal cell death (Jones et al., 1995; Booth et al., 2000). Axon contact with longitudinal glia is necessary for neuronal survival, but pioneer axons (the first ones to grow) are exempt (Booth et al., 2000). *Drosophila* homologs of vertebrate neurotrophins (called *DNT*s) have now been identified and are expressed at the CNS midline. When the *DNT*s are deleted, neuronal apoptosis is increased, confirming functional homology (Zhu et al., 2008).

Netrins are classical axon guidance cues that are best known for attracting growing axons to the CNS midline (Hedgecock et al., 1990; Serafini et al., 1994; Lai Wing Sun et al., 2011). In *Drosophila*, *Netrins* and *DNTs* share strikingly similar patterns of expression as both are expressed by the midline intermediate target and in target tissues such as muscles and the lamina of the optic lobe (Mitchell et al., 1996; Harris et al., 1996; Gong et al., 1999). Here, we demonstrate highly differential roles for the two closely related fly *Netrin* genes, *NetA* and *NetB*, with *NetB* appearing to be a neurotrophic factor and *NetA* appearing more neurotropic (affecting guidance) and even proapoptotic in some contexts. Overexpression of *NetB* is sufficient to rescue naturally occurring cell death. Surprisingly, inhibition of neuronal cell death is sufficient to restore the connectivity of the axon scaffold in *NetAB* mutants. Our data suggest that the *NetAB* mutant phenotype is the result of pioneer axon guidance defects amplified by subsequent cell death. Our results suggest that

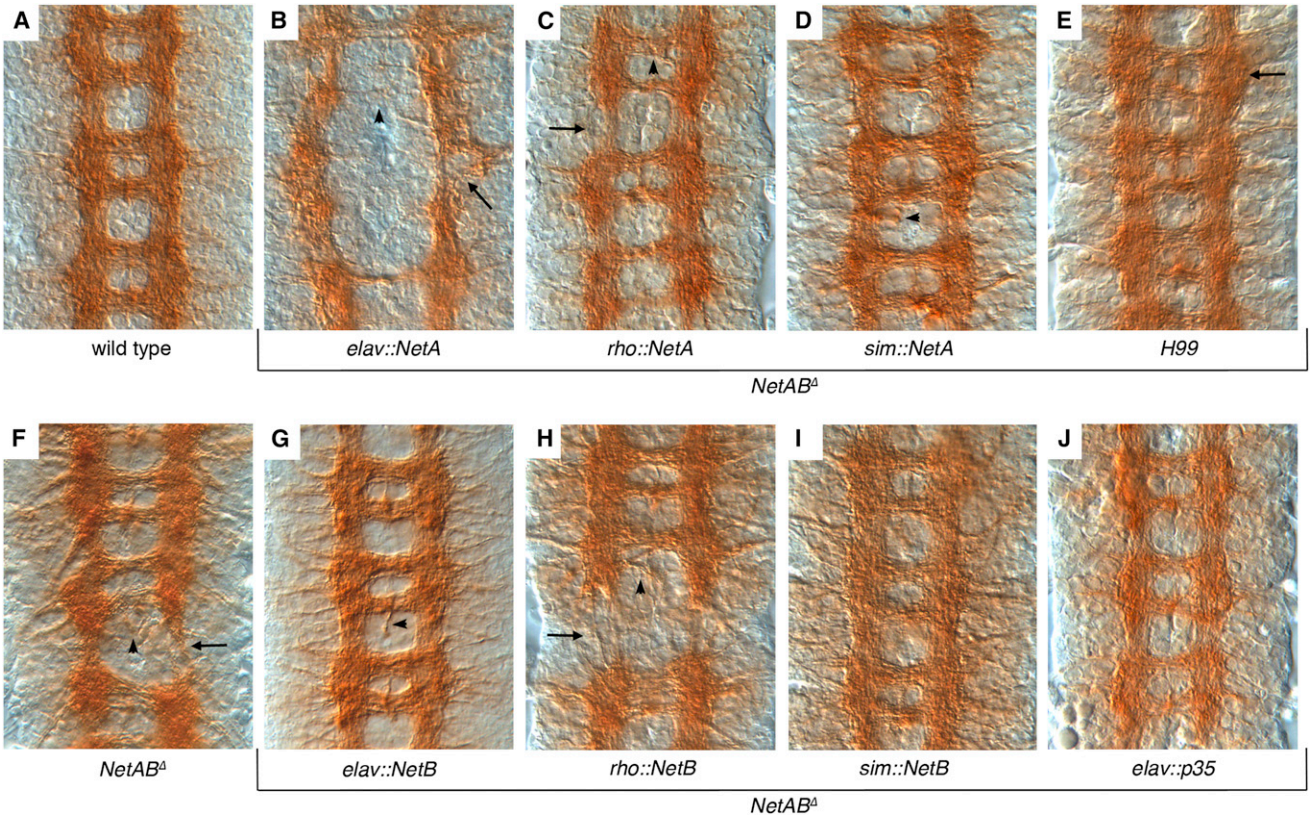

Figure 1. Rescue of *NetAB*$^{\Delta GN}$ Axon Scaffold Defects by Neuronal *NetB* Expression or Inhibition of Cell Death

Stage 16 embryonic ventral nerve cords stained with the BP102 monoclonal antibody to reveal the CNS axon scaffold (anterior at the top). *H99* represents one copy of the deletion encompassing the proapoptotic genes *hid*, *grim,* and *reaper* in the *NetAB*$^{\Delta GN}$ background. All other genetic notation represents one copy of *GAL4* and *UAS* transgenes in the *NetAB*$^{\Delta GN}$ background.

(A) Wild-type embryo showing the characteristic ladder-like pattern of the axon scaffold. (B) *NetAB*$^{\Delta GN}$ mutant with pan-neuronal expression of *NetA* under control of the *elav* promoter displaying disruption of commissural axons (arrowhead) and longitudinal tracts (arrow).

(C) *NetAB*$^{\Delta GN}$ mutant expressing *NetA* under control of the *rho* promoter (neuroectoderm and midline). Commissural (arrowhead) and longitudinal defects (arrow) are still visible.

(D) *NetAB*$^{\Delta GN}$ mutant expressing *NetA* under control of the *sim* midline promoter displaying phenotypic rescue, although minor defects are still visible (arrowhead).

(E) *NetAB*$^{\Delta GN}$ mutant heterozygous for the *H99* deficiency, which contains the proapoptotic genes *grim*, *reaper,* and *hid*. Commissural and longitudinal connectivity is rescued, although thickening of the longitudinals is observed (arrow).

(F) *NetAB*$^{\Delta GN}$ mutant displaying characteristic reduction of commissural axons (arrowhead) and longitudinal axons (arrow).

(G) *NetAB*$^{\Delta GN}$ mutant with pan-neuronal expression of *NetB* under control of the *elav* promoter displaying rescue of commissural and longitudinal axon defects, although misguided axons are still visible (arrowhead).

(H) *NetAB*$^{\Delta GN}$ mutant expressing *NetB* under control of the *rho* promoter displaying commissural (arrowhead) and longitudinal defects (arrow).

(I) *NetAB*$^{\Delta GN}$ mutant expressing *NetB* under control of the *sim* midline promoter displaying phenotypic rescue.

(J) *NetAB*$^{\Delta GN}$ mutant expressing the apoptosis inhibitor p35 in all postmitotic neurons, with rescue of midline and longitudinal defects.

See also Figure S1, and Tables S1 and S2.

caspase activity directly modulates growth cone guidance as well as mediating apoptosis.

RESULTS

Generation of an Adult Viable *NetAB* Double Mutant

The two *Drosophila Netrin* genes, *NetA* and *NetB*, are believed to be largely redundant in the CNS, necessitating the use of deletions that remove both genes to analyze their effects on development. The smallest deletion available, *NetAB*$^{\Delta MB23}$, deletes both genes and the intervening sequence (Brankatschk and Dickson, 2006). Genetic analysis suggested that the *NetAB*$^{\Delta MB23}$ chromosome carries additional mutations that synthetically interact with the *NetAB* deletion to decrease viability, and these were removed by recombination. The resulting stock, *NetAB*$^{\Delta GN}$, has greatly improved viability and can be maintained as homozygotes, albeit with some difficulty. The frequency of axon scaffold defects is unchanged in *NetAB*$^{\Delta GN}$ (Figure 1F; Table S1; Brankatschk and Dickson, 2006; Andrews et al., 2008) suggesting that the mutations removed did not affect axon guidance.

Pan-neuronal Expression of *NetB* Can Rescue *NetAB* Mutants

To confirm that the defects seen were due to the missing *Netrin* genes, the *NetAB*$^{\Delta GN}$ mutant was rescued by transgenic expression of *NetA* and *NetB* at the midline using the *single-minded* (*sim*) promoter (Figures 1D and 1I; p = 0.009, Fischer least significant difference [LSD] test). A second midline promoter (*rhomboid - rho*) gave more variable results and did not show a statistical difference from *NetAB*$^{\Delta GN}$ (Figures 1C and 1H; p = 0.26, Fischer LSD test). Nevertheless, *rho-NetB* expression is capable of rescuing behavioral defects in *NetAB*$^{\Delta GN}$ mutants (see below), suggesting that axonal connectivity might not be the only function of the *Netrins*. As a control, *Netrins* were expressed in all postmitotic neurons using the *elav* promoter, expecting this to further disrupt axon pathfinding due to the loss of midline positional information (Mitchell et al., 1996; Harris et al., 1996). *NetA* expression further disrupted axon guidance in *NetAB* mutants as expected (Figure 1B), but remarkably *NetB* expression produced a high degree of rescue of the CNS axon scaffold despite an absence of positional information (Figure 1G; p = 0.05, Tukey honestly significant difference [HSD] test).

Inhibition of Cell Death Rescues *NetAB* Mutants

Because Netrin-1 has been shown to act as a survival factor for commissural spinal cord neurons in mice (Furne et al., 2008), we reasoned that pan-neuronal expression of *NetB* might be inhibiting neuronal apoptosis. To inhibit cell death, we combined *NetAB*$^{\Delta GN}$ with the *H99* deficiency (White et al., 1994), which deletes the proapoptotic genes *grim, reaper,* and *hid*. This led to a strong rescue of the CNS axon scaffold (Figure 1E; Table S1; p < 0.0001, Fischer LSD test). To demonstrate that the cell death was neuronal, the viral apoptosis inhibitor *p35* (Hay et al., 1994) was expressed in all postmitotic neurons using the *elav* promoter. This also suppressed *Netrin* axon guidance defects (Figure 1G; Table S1; p = 0.028, Fischer LSD test). These results indicate that positional information is not strictly necessary for *Netrin* function. Other sources of positional information can attract axons in the absence of *NetA* and *NetB* (Brankatschk and Dickson, 2006; Andrews et al., 2008).

CNS neuronal apoptosis reaches its highest level at stage 14 and remains approximately constant until embryogenesis ends (Abrams et al., 1993; Rogulja-Ortmann et al., 2007). *NetAB*$^{\Delta GN}$ mutants display increased apoptosis during these stages (Figure 2), and this increase can be suppressed by pan-neuronal expression of *p35* or *NetB*. Pan-neuronal expression of *NetA* led to an intermediate phenotype (not statistically different from wild-type or *NetAB*$^{\Delta GN}$), suggesting that NetA may have indirect effects on neuronal survival. There are two known Netrin receptors in the fly: *fra* and *Dscam* (Kolodziej et al., 1996; Andrews et al., 2008). Levels of cell death were not increased in either mutant. *Dscam fra* double mutants do show a significant increase in VNC apoptosis, suggesting there may be functional overlap between the two Netrin receptors or that the disruptions to axon guidance indirectly lead to cell death.

To determine whether the Netrins are still required as navigational cues in the absence of cell death, we examined the SP1 neuron. Axonal defects were as previously reported (Andrews et al., 2008) and cell body positioning was slightly improved in *NetAB*$^{\Delta GN}$ mutants with blocked cell death (Table S2; Figures S1C and S1D; p = 0.02, Tukey HSD for *NetAB*$^{\Delta GN}$ *elavGAL4::UASp35*). These results suggest that Netrin positional information is required early in axonogenesis but the guidance defects in *NetAB* mutants are amplified by subsequent neuronal apoptosis.

NetB Functions as a Neurotrophic Factor

Neurotrophic factors are present in limited amounts in vivo, so increased expression should suppress naturally occurring cell death. To test this function for *NetB*, we expressed both *NetA* and *NetB* under control of a strong pan-neural promoter (*scaGAL4*) in a wild-type background. *NetA* had no effect on normally occurring apoptosis, but *NetB* dramatically reduced cell death in the VNC (Figure 2D; p = 0.0002, Tukey HSD). This result suggests that NetB is a neurotrophic factor.

Inhibiting Caspase Signaling in *eagle* EW Neurons Rescues Guidance but Not Death

To further understand the role of Netrins and survival in axon guidance, we examined the behavior of a small group of commissural neurons that can be identified by expression of the *eagle* (*eg*) transcription factor (Higashijima et al., 1996; Dittrich et al., 1997). Two populations of *eg*-expressing neurons are present in each abdominal hemisegment: the EW cluster and the more laterally located EG cluster (Figure 3A). The EW axons first extend in an anterior direction, then cross the midline in the posterior commissure of the next segment, while the EW axons grow straight toward the midline in the anterior commissure. Visualization of the *eg* neurons in *NetAB*$^{\Delta GN}$ embryos reveals a high level of disorganization in neuronal number and position and in axon pathfinding (Figure 3B). We confirmed the results of previous studies (Brankatschk and Dickson, 2006; Garbe et al., 2007) that midline crossing of EW axons is strongly disrupted in *NetAB* mutants (60% of segments relative to wild-type, p = 0.0001, Tukey HSD), while EG axons are affected to a lesser extent (20%, p = 0.04; Figures 3D and 3E). To test the effect of blocking cell death, we specifically expressed the *p35* inhibitor in *eg* neurons in *NetAB*$^{\Delta GN}$ mutants. Guidance of the EW commissure was significantly improved, with only 13% of segments displaying guidance errors (p = 0.0001 relative to *NetAB*$^{\Delta GN}$, Tukey HSD; Figure 3D). Rescue was not complete as EW commissure defects are still statistically different from wild-type (p = 0.03). Defects in the EG axons were not rescued (p = 0.12 relative to *NetAB*$^{\Delta GN}$, p = 0.88 relative to wild-type, Tukey HSD).

We also assessed the *eg* neurons for cell death in *NetAB*$^{\Delta GN}$ mutants. In wild-type embryos, each abdominal hemisegment has clusters of three to four EW and 10 to 12 EG cell bodies when visualized with *eg-GAL4* and either a *tau-lacZ* or *GFP* reporter. To quantify the number of neurons, we scored the presence of three or more cell bodies in an EW cluster and six or more in EG clusters as wild-type. *NetAB*$^{\Delta GN}$ mutants display a significant number of missing or reduced EW clusters (27%, p = 0.0004; Figure 3F), whereas EG clusters were statistically unaffected (p = 0.26; Figure 3G). Surprisingly, expression of *p35* in *eg* neurons did not rescue the missing EW neurons (Figure 3F) and *p35* expression increased EG cell death so that it

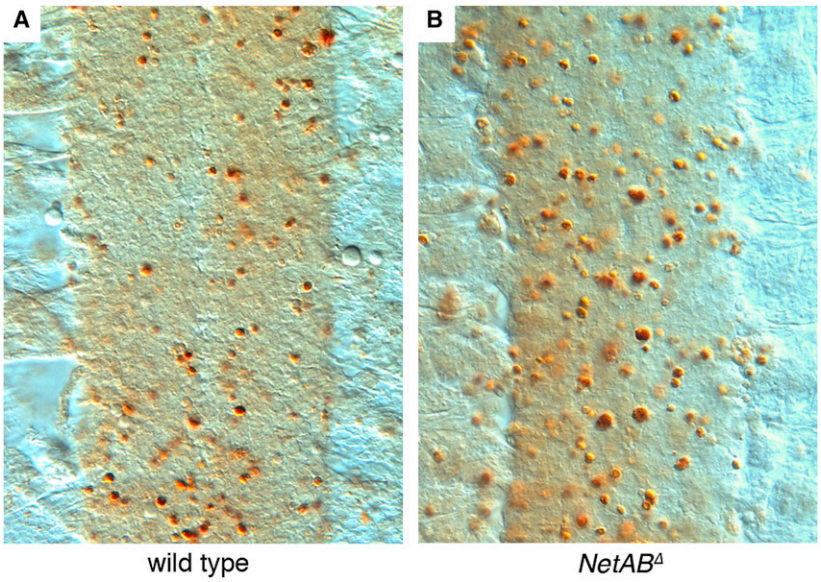

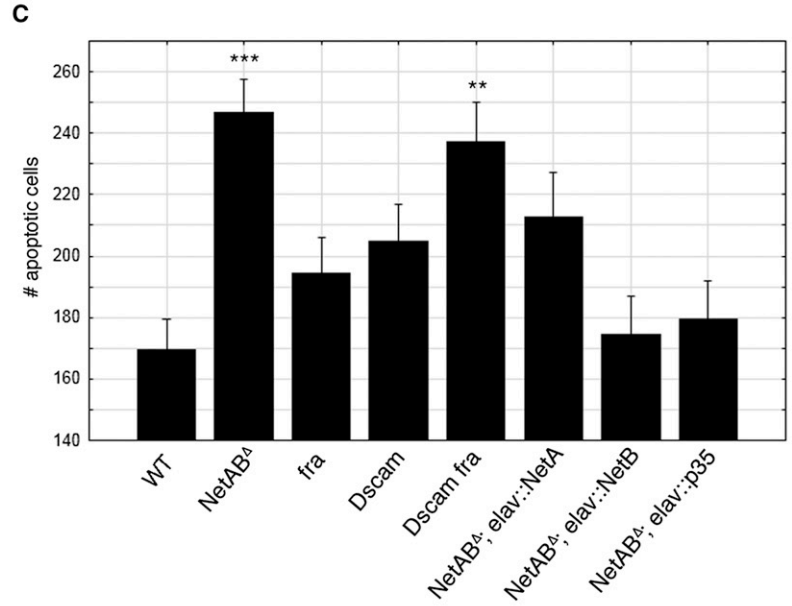

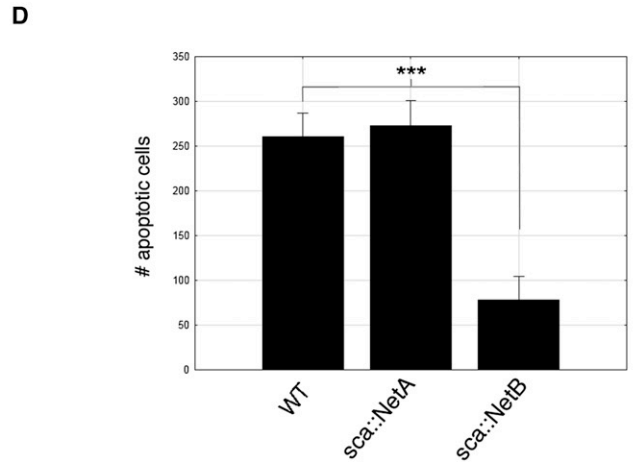

Figure 2. Apoptosis in *NetAB*$^{\Delta GN}$ and Wild-Type Ventral Nerve Cords Is Suppressed by *NetB*

Apoptosis in VNCs was measured by the TUNEL assay. Data shown are mean ±SEM; n ≥ 8 in all genotypes; p values in relation to wild-type (**p < 0.005, ***p < 0.0005, Tukey HSD within a one-way ANOVA.

(A) Wild-type embryos display stochastic patterns of apoptosis (brown nuclei).

(B) The number of apoptotic cells is visibly increased in *NetAB*$^{\Delta GN}$ mutant VNCs.

(C) Bar graphs represent mean number of apoptotic cells in all thoracic and abdominal segments of the VNC combined (11 segments total). *NetAB*$^{\Delta GN}$ mutants have significantly increased numbers of apoptotic cells. Individual mutants for the Netrin receptors *frazzled* (*fra*) and *Dscam* do not show an increase in apoptosis. However, *Dscam frazzled* (*Dscam fra*) double mutants show a significant increase in apoptosis relative to wild-type. Expression of *NetA* pan-neuronally in *NetAB* mutants fails to significantly reduce apoptosis (*NetAB*$^{\Delta GN}$; *elav::NetA*), but expression of *NetB* pan-neuronally does significantly rescue (*NetAB*$^{\Delta GN}$; *elav::NetB*, p < 0.0005), as does inhibiting apoptosis by expression of *p35* (*NetAB*$^{\Delta GN}$; *elav::p35*, p < 0.0005).

(D) Overexpression of *Netrins* in wild-type. Expression of *NetA* under control of the pan-neuronal driver *scabrous* (*sca::NetA*) fails to significantly change cell death from wild-type levels in the VNC. Expression of *NetB* (*sca::NetB*) significantly decreases apoptosis.

is statistically different from wild-type (p = 0.004). This separation of apoptotic and guidance activities is potentially explained by the inability of *p35* to inhibit certain caspases including Dronc, a key embryonic regulator (Meier et al., 2000; Hawkins et al., 2000). Alternatively, the *eg* promoter used may not express with sufficient strength or appropriate timing. In summary, the EW neurons display guidance and cell survival errors in *NetAB*$^{\Delta GN}$ mutants. The guidance errors can be significantly but not completely rescued by *p35* expression without rescue of cell death.

NetA and *NetB* Have Opposing Effects in the Fly Eye

The fly eye is a widely used system to examine the effects of mutations on cell death (McCall et al., 2009). Expression of the proapoptotic gene *hid* sensitizes the eye to further perturbations in cell death (Figure 4), and the size of the eye indicates the level of neuronal death occurring in the retina. Reduction of *NetA* activity by loss-of-function mutation or eye-specific RNA interference (data not shown) suppresses the *hid* small-eye phenotype, suggesting that *NetA* is proapoptotic in this context (Figure 4B; p = 0.00018, Tukey HSD within a one-way ANOVA). In contrast, in the *NetB* mutant background, the size of the eye is reduced compared to wild-type (Figure 4C; p = 0.012), suggesting an increase in cell death in the absence of *NetB*. Eye size is similar to the control in the *NetAB* double mutant, and thus *NetA* and *NetB* seem to balance each other out in this system (Figure 4D). These differential effects are reminiscent of the dissimilarities observed with pan-neuronal expression of *NetA* or *NetB* in the embryo. However, in this context, *NetA* may be acting as a proapoptotic signal in contrast to *NetB*'s role as a neuronal survival factor.

Inhibition of Apoptosis Suppresses *NetAB* Behavioral Deficits

Netrin/*unc-6* mutants were first isolated in *C. elegans* due to the uncoordinated movement of adults (Hedgecock et al., 1990). Adult *NetAB*$^{\Delta GN}$ flies have an uncoordinated phenotype that we used to functionally test the role of cell death. Midline cells persist until a point halfway through pupation and are proposed to continue to guide growing axons (Awad and Truman, 1997). Continued expression of midline genes supports this model (Lanoue and Jacobs, 1999; Pielage et al., 2002; Tayler et al., 2004) and allowed us to test whether adult behavioral phenotypes could be rescued. The tendency of flies to climb the wall of a vial after being tapped to the bottom (negative geotaxis) is a widely used assay of neural function (Gargano et al., 2005). *NetAB*$^{\Delta GN}$ flies show consistent defects in this assay, but are rescued by midline expression of *NetA* or *NetB* by the *sim* promoter or *NetB* by the *rho* promoter (Figure 5A). Blocking apoptosis through neuronal expression of *p35* improved the performance of *NetAB*$^{\Delta GN}$ flies (Figure 5B; p < 0.005, Tukey HSD). The *H99* deficiency did not rescue, perhaps due to effects on nonneural tissues.

A second standard behavioral assay in flies is locomotor reactivity (Jordan et al., 2007). The overall locomotion of *NetAB*$^{\Delta GN}$ mutants was assayed by monitoring their activity over a period of 45 s after a mechanical startle (tapping each fly to the bottom of the vial) and consistent reductions in activity were noted. Locomotor reactivity could be improved by midline or neuronal expression of *NetA* but not *NetB* (Figure 5C). Locomotor performance was rescued by the *H99* deficiency but not neuronal expression of *p35* (Figure 5D). *H99* may be affecting the survival of both neural and nonneural tissues, as Netrins are expressed outside the nervous system (Harris et al., 1996; Mitchell et al., 1996), or some of the affected neurons are insensitive to p35 as is seen for the EW neurons. Despite the inherent complexity of behavioral assays, our results confirm that promoting cell survival is an important aspect of *Netrin* function.

DISCUSSION

The Role of Netrins in CNS Midline Guidance

In a wild-type embryo, both *NetA* and *NetB* act to attract axons to the CNS midline, and expression of either *Netrin* at the midline is sufficient to rescue the *NetAB* axon scaffold defects (Mitchell et al., 1996; Harris et al., 1996; Brankatschk and Dickson, 2006; Figure 1). Because *NetA* lacks neurotrophic activity but can rescue guidance on its own, death in *NetAB* mutants may be a consequence of axons failing to contact the midline. This idea is supported by the report that a membrane-tethered form of *NetB* integrated into the endogenous *NetB* locus is capable of rescuing the *NetAB* phenotype (Brankatschk and Dickson, 2006). The *Netrins* are also required for positioning of the longitudinal glia that supply trophic signals to axons (von Hilchen et al., 2010). Therefore, a combination of initial guidance and glial positioning errors in *NetAB* mutants may be amplified by subsequent cell death. In summary, axon guidance in the *Drosophila* VNC does not simply rely on navigational information supplied by cues, but is supported by glial-derived trophic factors expressed by the intermediate targets of navigating axons including longitudinal and midline glia.

Apoptosis in *Netrin* Mutants

Why was CNS cell death not previously detected in *NetAB* mutants? Analysis of cell fate in *NetAB* mutants focused on markers for subsets of neurons including the pioneers (Mitchell et al., 1996; Harris et al., 1996; Andrews et al., 2008), which do not have requirements for trophic support (Booth et al., 2000). Apoptosis increases with the maturity of the embryonic nervous system, so missing neurons may not be apparent when analysis is done at earlier stages of development. Like *DNT* mutants (Zhu et al., 2008), *NetAB* embryos show a relatively small increase in cell death, so the probability of observing a particular missing cell may be low. Finally, the disorganized nature of the *NetAB* CNS may have masked cell death due to altered neuronal positioning (see Figure 3B). The highly variable nature of *NetAB* mutant phenotypes (Mitchell et al., 1996; Harris et al., 1996; Brankatschk and Dickson, 2006; Andrews et al., 2008) can also be accounted for by the stochastic nature of cell death in the VNC as different neurons may die in different individuals.

Netrins as Neuronal Survival Factors during Axon Outgrowth

The role of Netrin-1 as a neuronal survival factor in the spinal cord remains under debate as conflicting results have been obtained (Williams et al., 2006b; Furne et al., 2008; reviewed in Lai Wing

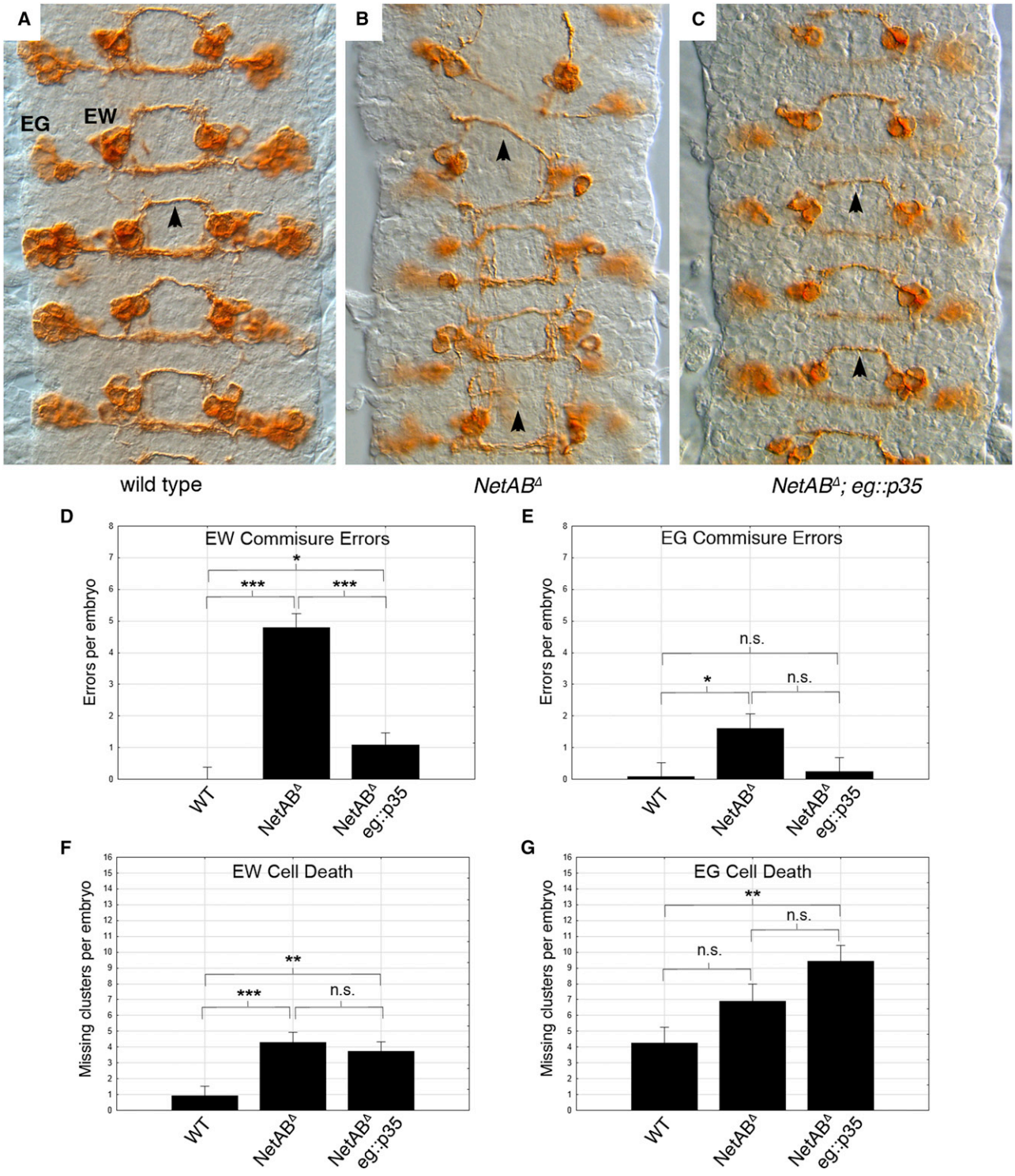

Figure 3. Blocking Caspase Activity in *eg* Neurons in *NetAB$^{\Delta GN}$* Mutants Rescues Axon Guidance of These Neurons without Rescuing Cell Death

Stage 16 ventral nerve cords labeled by driving *tau-LacZ* in neurons expressing *eg* (*elGAL4::UAStauLacZ*), stained with anti-βgal antibody (A–C). Two populations are shown: EW (medial) and EG (lateral). In all graphs, data shown are mean ±SEM; *p < 0.05; **p < 0.005; ***p < 0.0005, Tukey HSD within a one-way ANOVA. n = 12 for wild-type and *NetAB$^{\Delta GN}$;egGAL::UASp35;* n = 10 for *NetAB$^{\Delta GN}$* (D–G).

(A) Wild-type embryos show robust label of EW and EG cell bodies. Each population sends a commissural bundle to meet and adhere to the corresponding contralateral population (arrowhead).

(legend continued on next page)

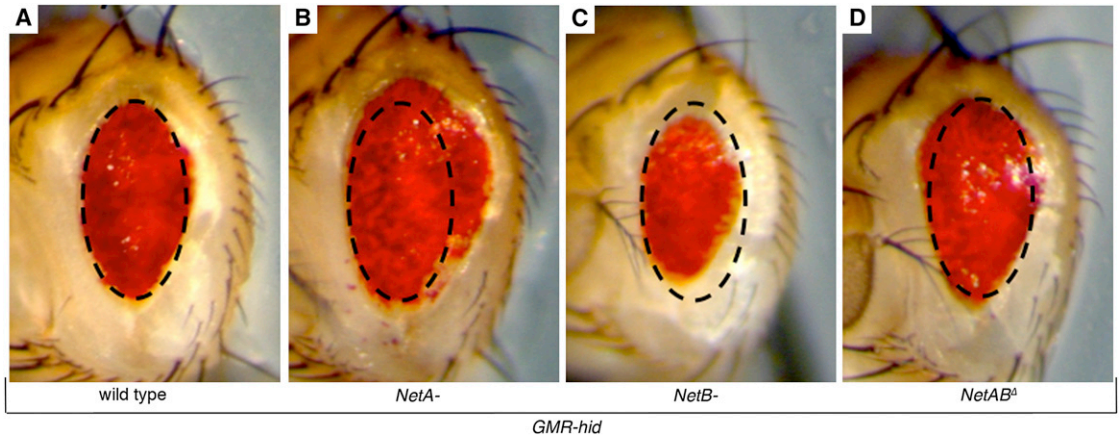

Figure 4. Differential Effects of *NetA* and *NetB* on Eyes Sensitized for Cell Death

Adult male *Drosophila* eyes expressing the proapoptotic gene *hid* photographed at ×85 magnification.

(A) *hid* expression in the fly eye increases cell death, leading to a reduced eye size represented by the dotted circle.

(B) Removal of *NetA* activity using the $NetA^{\Delta}$ deletion partially suppresses cell death, increasing eye size.

(C) Removal of *NetB* activity using the $NetB^{\Delta}$ deletion increases cell death, further reducing the eye size.

(D) Removal of both *NetA* and *NetB* simultaneously using the $NetAB^{\Delta MB23}$ deletion has little effect on the *hid* eye-size phenotype.

Sun et al., 2011). The occurrence of cell death in fly *NetAB* mutants raises the possibility that neurotrophic activity is an evolutionarily conserved function of Netrins. The fly embryonic CNS provides an assay system to functionally test Netrins from other species for neurotrophic activity in vivo. Classically, the axonal target tissue produces neurotrophic factors. An increasing number of examples are now known where intermediate targets supply neurotrophic factors, a phenomenon termed *en passant* or pretarget neurotrophic action (Wang and Tessier-Lavigne, 1999; Usui et al., 2012; Kuruvilla et al., 2004; Furne et al., 2008). Because NetB is expressed by the CNS midline intermediate target as well as in final targets such as muscles, it may function as an *en passant* neurotrophic factor.

Nonapoptotic Caspase Signaling in Single Neurons

Cell death during development of the fly embryonic CNS is estimated to be as high as 50% (White et al., 1994). Therefore, a possible explanation for the suppression of the *NetAB* midline-crossing phenotype by inhibiting cell death is that the rescue of cells fated to die compensates for guidance errors by other axons. Midline crossing appears to be the default pathway when trophic constraints on neurons are removed (Kinrade et al., 2001), so axons from rescued cells could be expected to cross the midline and mask guidance defects of other neurons. Our results with the EW neurons strongly argue against this scenario. Expression of *p35* does not rescue the EW cell-death phenotype, so trophic constraints are still present yet correct guidance is largely restored. The activity of p35 is cell autonomous, so modulation of caspase activity within a single neuron must be via nonapoptotic effects.

Caspase Signaling in Axon Guidance

Caspases are central players in apoptosis, but nonapoptotic functions of caspases are becoming increasingly apparent (Feinstein-Rotkopf and Arama, 2009). In *Drosophila*, dendritic pruning requires local activation of caspase activity by degradation of the caspase inhibitor DIAP1 (Kuo et al., 2006; Williams et al., 2006a; Rumpf et al., 2011). Mutation of DIAP1 in the fly ovary leads to border cell-migration defects in the absence of excess cell death (Geisbrecht and Montell, 2004). The fly *IKKε* (*ik2*) kinase inhibits actin polymerization by regulation of DIAP1 (Oshima et al., 2006) and can inactivate DIAP1 by direct phosphorylation

(B) $NetAB^{\Delta GN}$ mutants display significantly disorganized wiring of *eg* neurons, with many commissures absent from both the EW and EG populations (arrowheads). Some cell bodies are also missing.

(C) Expression of *p35* in *eg* neurons in $NetAB^{\Delta GN}$ mutants rescues the commissural guidance of the *eg*-expressing neurons (arrowheads). EG populations are out of the plane of focus, so appear weakly labeled.

(D) $NetAB^{\Delta GN}$ mutants display commissural guidance defects in the EW neurons (out of eight possible commissures). Expressing *p35* in *eg* neurons in $NetAB^{\Delta GN}$ mutants ($NetAB^{\Delta GN}$; *eg::p35*) significantly reduces EW guidance errors, though this number is still significantly different from wild-type.

(E) $NetAB^{\Delta GN}$ mutants display commissural guidance defects in the EG neurons (out of eight possible commissures). Expressing *p35* in *eg* neurons in $NetAB^{\Delta GN}$ mutants ($NetAB^{\Delta GN}$; *eg::p35*) appears to rescue this guidance error, but this number is not statistically different from $NetAB^{\Delta GN}$ or wild-type ($p = 0.12$ and $p = 0.88$, respectively).

(F) $NetAB^{\Delta GN}$ mutants display an increase in cell death in EW neurons over wild-type (two per hemisegment, 16 total possible). Expressing *p35* in *eg* neurons fails to rescue this cell death.

(G) $NetAB^{\Delta GN}$ mutants fail to display a significant increase in cell death in EG neurons over wild-type (two per hemisegment, 16 total possible, $p = 0.26$). However, expressing *p35* in *eg* neurons causes the cell death to be significantly increased compared to wild-type, though this number is not statistically different from $NetAB^{\Delta GN}$ ($p = 0.21$).

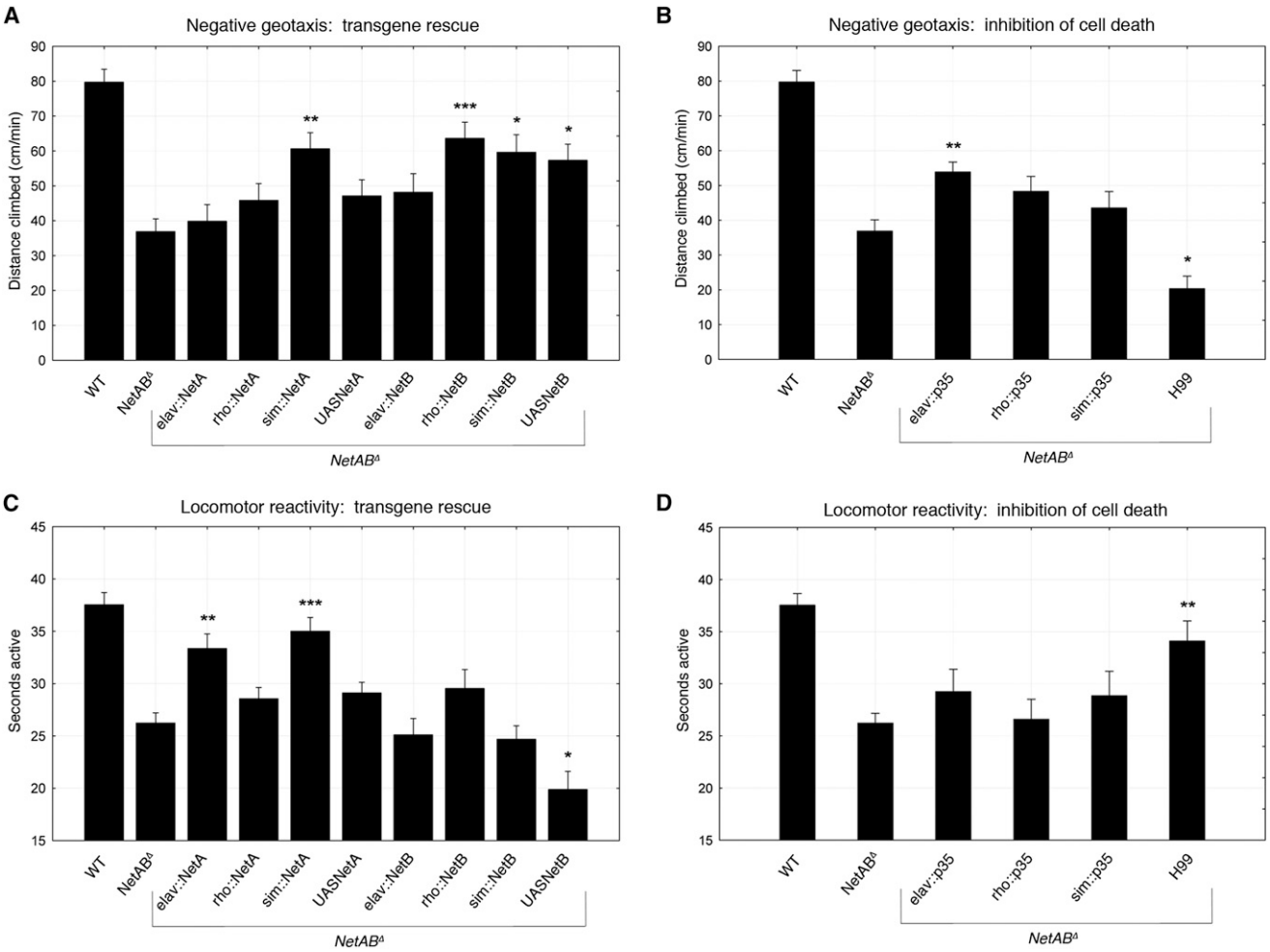

Figure 5. Specific Behavioral Defects in Adult *NetAB*$^{\Delta GN}$ Mutants Are Rescued by Transgenic *Netrin* Expression and Inhibition of Cell Death

In all graphs, all columns are mutant for *NetAB*$^{\Delta GN}$ except for the left-hand column, which is wild-type. In all graphs, data are shown as mean ±SEM; *p < 0.05; **p < 0.005; ***p < 0.0005. Statistical differences are reported with respect to the *NetAB*$^{\Delta GN}$ mutant phenotype. *H99* represents one copy of the deletion encompassing *hid, grim,* and *reaper*. All other genetic notation represents one copy of *GAL4* and *UAS* transgenes in the *NetAB*$^{\Delta GN}$ background.

(A and B) Bar graphs represent the mean distance climbed upward per animal (n ≥ 10 in all genotypes, only males tested, and all p values in relation to *NetAB*$^{\Delta GN}$ mutants). *NetAB*$^{\Delta GN}$ mutants climb significantly less than wild-type (p = 0.00001). (A) Midline *Netrin* expression rescues negative geotaxis in *Netrin* mutants either by *NetA* expression at the midline under control of *sim-GAL4* or by *NetB* expression at the midline using either *rho-GAL4* or *sim-GAL4*. Though *Netrin* mutants possessing one copy *UAS-dNetB* transgene were significantly different from *Netrin* mutants alone, this result is explained by one fly that performed remarkably better than all wild-type. (B) Inhibiting cell death in neurons by expressing *p35* under control of *elav-GAL4* rescues negative geotaxis in *NetAB*$^{\Delta GN}$ mutants. Inhibiting cell death in the entire animal with the *H99* deletion further disrupts *NetAB*$^{\Delta GN}$ negative geotaxis.

(C and D) Bar graphs represent the mean amount of time spent ambling out of 45 s postmechanical disturbance (n ≥ 20 in all genotypes, both sexes tested, and all p values in relation to *NetAB*$^{\Delta GN}$ mutants). Locomotor reactivity to a mechanical disturbance is significantly reduced in *NetAB*$^{\Delta GN}$ mutants compared to wild-type (p = 0.00001). (C) Locomotor reactivity defects of *Netrin* mutants are rescued by expression of *NetA* in neurons with *elav-GAL4* or at the midline with *sim-GAL4*. *NetB* expression under control of each of the drivers tested failed to affect locomotor reactivity, although flies carrying the *NetB* transgene were statistically less mobile, suggesting the transgene could have leaky expression. Presence of the *UAS-dNetB* transgene alone significantly decreased locomotor reactivity of *Netrin* mutants. (D) Locomotor reactivity is rescued by inhibiting cell death in the entire animal with the *H99* deletion.

(Kuranaga et al., 2006). Vertebrate caspases can promote actin depolymerization by modulating cofilin activity (Li et al., 2007). Because axon outgrowth and chemoattraction requires actin polymerization (Lowery and Van Vactor, 2009), it seems plausible that caspase activation could hinder these processes by inhibiting actin polymerization. Conversely, inhibition of caspase activation could stimulate axon outgrowth in the absence of Netrins, allowing axons to respond to other unidentified midline attractants. It has been shown that in *NetAB* mutants, axons still orient and grow toward the midline but fail to cross (Brankatschk and Dickson, 2006); inhibition of caspase activity might provide sufficient stimulus to overcome this hurdle.

A previous study demonstrated that caspase activation is necessary for the chemotropic response of *Xenopus* retinal growth cones to Netrin-1 (Campbell and Holt, 2003). This contrasts with our results suggesting that caspase inhibition is

important for the response to Netrin. In vitro experiments have demonstrated that cells expressing the DCC Netrin receptor only activate caspase signaling in the absence of Netrin (Forcet et al., 2001). This suggests that specific cellular and developmental contexts will determine how the caspase machinery responds to Netrins. In vertebrates, DCC binds caspase-3 and caspase-9 at different sites within DCC's cytoplasmic domain, providing a direct link between a Netrin receptor and the caspase machinery (Forcet et al., 2001). DCC is also a caspase substrate (Mehlen et al., 1998), but the cleavage site is not conserved in *Drosophila* (Furne et al., 2008). The fly DCC homolog, *fra*, does not increase cell death when mutated, suggesting that the neurotrophic function of NetB is mediated by an unidentified receptor. The exact binding sites of caspases in DCC are not known, but motifs are highly conserved between Fra and DCC (Kolodziej et al., 1996), so caspase binding may be conserved. It is possible that both *NetA* and *NetB* finely modulate caspase signaling to effect cytoskeletal changes, but only *NetB* has sufficient strength of inhibition to prevent apoptosis. NetB may inhibit caspase activity to promote both attraction and neuronal survival. The differential effects of *NetA* and *NetB* offer the opportunity to further understand how accurate nervous system connectivity is achieved.

Summary

Our results demonstrate that cell death is an integral part of the *Drosophila Netrin* CNS phenotype and that *NetB* functions as a neurotrophic factor. We report the surprising observation that inhibiting apoptotic signaling can restore axon attraction to the midline, suggesting that local caspase activity in the growth cone modulates pathfinding. The generation of an adult viable *NetAB* mutant provides a functional readout of nervous system development and confirms that apoptotic signaling plays a role in Netrin function. Our data support models in which coupling neuronal survival with guidance could ensure accurate neuronal connectivity, as axons making navigational errors would be eliminated (Mehlen and Furne, 2005; Vanderhaeghen and Cheng, 2010).

EXPERIMENTAL PROCEDURES

Drosophila Stocks and Maintenance

All stocks were obtained from the Bloomington Stock Center at Indiana University or, if unavailable, from the laboratories listed in Acknowledgments. The $NetAB^{\Delta GN}$ stock was maintained as both a homozygous and a balanced stock over FM7. The following stocks were used to generate genotypes for analysis: (1) *w- nonisogenic (Exelixis);* (2) $NetAB^{\Delta GN}$*/FM7 actβgal;* (3) $NetAB^{\Delta GN}$*/FM7 actβgal; elav-GAL4;* (4) $NetAB^{\Delta GN}$*/FM7 actβgal; sim-GAL4;* (5) $NetAB^{\Delta GN}$*/FM7 actβgal; rho-GAL;* (6) $NetAB^{\Delta GN}$*/FM7 actβgal; UAS-dNetA;* (7) $NetAB^{\Delta GN}$*/FM7 actβgal; UAS-dNetB;* (8) $NetAB^{\Delta GN}$*/FM7 actβgal; UAS-p35;* (9) *H99/TM3*; (10) fra^4 */ CyOWgβ;* (11) *Dscam/CyO wgβgal;* (12) fra^4*, Dscam/CyO wgβ;* (13) *UAS-dNetA;* (14) *UAS-dNetB;* (15) *eg-GAL4/TM3;* (16) *UAS-tau-lacZ/CyO wgβgal;* (16) $NetAB^{\Delta MB23}$/FM7; (17) $NetA^{\Delta}$; (18) $NetB^{\Delta}$; and (19) *sca-GAL4.*

Immunohistochemistry

Immunohistochemistry was performed as previously described (Patel, 1994). The following primary antibodies were used: (1) BP102 (Developmental Studies Hybridoma Bank [DSHB], 1:10); (2) anti-β-galactosidase (anti-β-gal; MP Biomedicals, 1:10,000); and (3) anti-Connectin (DSHB, 1:5). Anti-Connectin was stained according to Andrews et al. (2008) and enhanced with Vectastain (Vector Labs).

Commissural Analysis in the VNC

Commissural and longitudinal guidance was assessed using BP102 staining of late stage 15 and stage 16 embryos. The anterior and posterior commissures and the left and right hand longitudinals were scored in the three thoracic and eight abdominal segments as normal, reduced, absent, or other and then pooled per genotype. Table S1 summarizes the percent observed of each criterion. Statistics are reported comparing only normal to defective morphology among genotypes.

Analysis of *eg* Neurons

To analyze *eg*-expressing neurons, *UAS-tau-lacZ* was expressed under the control of *eg-GAL4* in wild-type and $NetAB^{\Delta GN}$ mutants. The neurons were visualized by staining with anti-β-gal antibody enhanced with Vectastain. Simultaneous expression of *UAS-p35* in the $NetAB^{\Delta GN}$ mutants was used to block caspase activation. Exact determination of the number of *eg* positive cell bodies present is challenging, especially in *NetAB* mutants, so we devised a scoring system to count the number of cells present in the abdominal segments. EW (medial and anterior) clusters normally contain four cell bodies. If an EW cluster contained more than two cells, it was scored as a "1"; if the cluster had two cells or fewer, it was scored as a "0." Each segment has two clusters, so the maximum score per segment is "2," and with eight abdominal segments scored, the maximum score per embryo is "16." The EG (lateral and posterior) population was scored similarly, but in this case, because the EG clusters normally contain 10 to 12 cell bodies, the criterion was six or more cells on each side to receive a score of "1." As before, a completely wild-type embryo will generate a score of "16." We believe that prior studies may have missed the missing neurons in part because of the variability in position and number of cell bodies, and the scoring system accurately discriminates between wild-type and mutants. EW and EG commissures were scored simply as present or absent (eight commissures of each neuronal population per embryo), and any abnormal pathfinding was noted, though not scored. Statistics were reported separately for EW and EG populations.

TUNEL Assay

Stage 15–17 embryos were fixed as for immunohistochemistry in 3.7% formaldehyde and rehydrated in four steps after being devitellinized in methanol. To detect balancer chromosomes, anti-β-gal staining was performed prior to the TUNEL procedure. Embryos were treated with Proteinase K (10 μg/ml) for 5 min, washed thoroughly, refixed, and incubated in freshly prepared citrate buffer (100 mM sodium citrate/0.1% Triton X) at 65°C for 30 min. After washing, the embryos were incubated in TUNEL reaction buffer (30 mM Tris/HCl, 140 mM sodium cacodylate, and 1 mM $CoCl_2$) at 37°C for 30 min and then reacted using the Terminal deoxynucleotidyl transferase reagents from the Roche in situ cell death detection POD kit. Staining was visualized with an anti-fluorescein antibody conjugated to horseradish peroxidase and diaminobenzidine development. Small volumes (50–100 μl of embryos) were incubated for 30 min at 37°C. Embryos used for analysis in Figures 2A–2C had their VNCs dissected and photographed in two different planes of focus, converted to grayscale, and contrast enhanced in Adobe Photoshop. The TUNEL-positive nuclei were then counted using VisionWorksLS colony-counting software. Duplicate cells represented in both planes of focus were subtracted from total. For the analysis in Figure 2D, images of dissected VNCs were taken in multiple planes of focus using bright field microscopy in an attempt to capture every labeled cell in the VNC. Labeled cells were counted in ImageJ by an experimenter unaware of the conditions of the experiment and blind to genotype. Duplicate cells represented in more than one plane of focus were subtracted from total. Due to inherent variability in the results obtained with TUNEL staining, experiments were done in batches and the results may not be directly comparable between experiments done at different times (e.g., Figures 2C and 2D).

Eye Apoptosis Assay

Drosophila heads were dissected and mounted on 1μl micropipettes using rubber cement. The heads were submerged in water and imaged using a Zeiss

Discovery V12 dissecting microscope equipped with a color camera and a plan S 1.0X FWD 81 mm objective. All images were acquired at ×85 magnification and processed identically.

Locomotor Activity

This assay was modeled after Jordan et al. (2007). Briefly, 1-day-old flies of each genotype and sex (collected and housed individually at 25°C, constant humidity) were measured by counting the number of seconds the fly spent walking out of the 45 s following a mechanical disturbance (tapping flies to the bottom of the vial) at room temperature. The experimenter was blind to genotype during recording.

Negative Geotaxis

Individual flies were assayed as described in Gargano et al. (2005). Briefly, male flies 1–2 days old were placed individually in small graduated serological pipettes using a mouth pipette system to avoid anaesthetization. Flies were mechanically jolted to the bottom of 10 ml serological pipettes and their upward walking distance was recorded for 1 min. Flies were jolted back to the bottom as necessary if they approached the top during each trial. Each fly experienced three 1 min trial periods, each interspersed with a 1 min rest period. The experimenter was blind to genotype during recording and video analysis.

Statistical Analysis

Statistical analysis was performed using Statistica (Statsoft). All data are expressed as group means ±SEM. On TUNEL, eye apoptosis, and locomotor assays, statistical analysis was performed using a Tukey HSD test within a one-way ANOVA. For negative geotaxis, we performed a Tukey HSD test within a repeated-measures ANOVA. For the TUNEL assay, population counts of cell death were found to marginally fall within a normal distribution. Therefore, statistics were confirmed using a Kruskal-Wallis one-way analysis of variance. All statistical significance was maintained with this nonparametric test, so only p values for the more common Tukey HSD test were reported. For commissural analysis on the BP102 antibody labels and *eg* populations, data from each commissure were categorized as either normal or defective and expressed as a ratio per embryo. Arcsine transformation was then performed to satisfy assumptions of analysis. For BP102, statistical analysis was performed using the Fisher LSD test because models of midline guidance, previous publications (Harris et al., 1996; Mitchell et al., 1996; Brankatschk and Dickson, 2006), and our prior hypotheses suggested specific outcomes. *NetAB$^{\Delta GN}$; elavGAL4::UASdNetB* failed to match prior hypotheses; therefore, the Tukey HSD value is reported for these data. On all assays, except where noted, p values are reported compared to the *NetAB$^{\Delta GN}$* mutant. Statistical significance was set at $p < 0.05$.

SUPPLEMENTAL INFORMATION

Supplemental Information includes one figure and two tables and can be found with this article online at http://dx.doi.org/10.1016/j.celrep.2013.02.017.

LICENSING INFORMATION

ACKNOWLEDGMENTS

We thank B. Dickson, M. Brankatschk, B. Altenhein, E. Giniger, M. Seeger, and A. DiAntonio for stocks and reagents. We thank K. McCall, T. Pritchett, A. Bergmann, A. Hidalgo, and B. Olofosson for advice on cell death staining, J. Goldstein for advice on the negative geotaxis assay, and M. Forrister and V. Pravosudov for help with statistical analysis. We thank G. Andrews, D. Tailor, M. Bowser, S. Hugdal, and T. Gillis for advice and technical assistance. We thank P. Berninsone, B. Bjorke, S. Clark, E. Justice, A. Keene, G. Mastick, A. van der Linden, and C. von Bartheld and unidentified reviewers for comments on the manuscript. Antibodies were obtained from the DSHB developed under the auspices of the NICHD and maintained by the University of Iowa. This project was supported by grants from the National Science Foundation (IOS-1052555), National Center for Research Resources (P20RR016464, 5P20RR024210), and the National Institute of General Medical Sciences (8 P20 GM103554) from the National Institutes of Health (T.K.) and a Klingenstein Fellowship Award in the Neurosciences (J.C.C.).

Received: June 13, 2012
Revised: January 14, 2013
Accepted: February 14, 2013
Published: March 14, 2013

REFERENCES

Abrams, J.M., White, K., Fessler, L.I., and Steller, H. (1993). Programmed cell death during Drosophila embryogenesis. Development *117*, 29–43.

Andrews, G.L., Tanglao, S., Farmer, W.T., Morin, S., Brotman, S., Berberoglu, M.A., Price, H., Fernandez, G.C., Mastick, G.S., Charron, F., and Kidd, T. (2008). Dscam guides embryonic axons by Netrin-dependent and -independent functions. Development *135*, 3839–3848.

Awad, T.A., and Truman, J.W. (1997). Postembryonic development of the midline glia in the CNS of Drosophila: proliferation, programmed cell death, and endocrine regulation. Dev. Biol. *187*, 283–297.

Baker, N.E., and Yu, S.Y. (2001). The EGF receptor defines domains of cell cycle progression and survival to regulate cell number in the developing Drosophila eye. Cell *104*, 699–708.

Bergmann, A., Agapite, J., McCall, K., and Steller, H. (1998). The Drosophila gene hid is a direct molecular target of Ras-dependent survival signaling. Cell *95*, 331–341.

Bergmann, A., Tugentman, M., Shilo, B.Z., and Steller, H. (2002). Regulation of cell number by MAPK-dependent control of apoptosis: a mechanism for trophic survival signaling. Dev. Cell *2*, 159–170.

Booth, G.E., Kinrade, E.F.V., and Hidalgo, A. (2000). Glia maintain follower neuron survival during Drosophila CNS development. Development *127*, 237–244.

Brankatschk, M., and Dickson, B.J. (2006). Netrins guide Drosophila commissural axons at short range. Nat. Neurosci. *9*, 188–194.

Buchanan, R.L., and Benzer, S. (1993). Defective glia in the Drosophila brain degeneration mutant drop-dead. Neuron *10*, 839–850.

Campbell, D.S., and Holt, C.E. (2003). Apoptotic pathway and MAPKs differentially regulate chemotropic responses of retinal growth cones. Neuron *37*, 939–952.

Campos, A.R., Fischbach, K.F., and Steller, H. (1992). Survival of photoreceptor neurons in the compound eye of Drosophila depends on connections with the optic ganglia. Development *114*, 355–366.

Dearborn, R., Jr., and Kunes, S. (2004). An axon scaffold induced by retinal axons directs glia to destinations in the Drosophila optic lobe. Development *131*, 2291–2303.

Dittrich, R., Bossing, T., Gould, A.P., Technau, G.M., and Urban, J. (1997). The differentiation of the serotonergic neurons in the Drosophila ventral nerve cord depends on the combined function of the zinc finger proteins Eagle and Huckebein. Development *124*, 2515–2525.

Domínguez, M., Wasserman, J.D., and Freeman, M. (1998). Multiple functions of the EGF receptor in Drosophila eye development. Curr. Biol. *8*, 1039–1048.

Feinstein-Rotkopf, Y., and Arama, E. (2009). Can't live without them, can live with them: roles of caspases during vital cellular processes. Apoptosis *14*, 980–995.

Forcet, C., Ye, X., Granger, L., Corset, V., Shin, H., Bredesen, D.E., and Mehlen, P. (2001). The dependence receptor DCC (deleted in colorectal cancer) defines an alternative mechanism for caspase activation. Proc. Natl. Acad. Sci. USA *96*, 3416–3421.

Furne, C., Rama, N., Corset, V., Chédotal, A., and Mehlen, P. (2008). Netrin-1 is a survival factor during commissural neuron navigation. Proc. Natl. Acad. Sci. USA *105*, 14465–14470.

Garbe, D.S., O'Donnell, M., and Bashaw, G.J. (2007). Cytoplasmic domain requirements for Frazzled-mediated attractive axon turning at the Drosophila midline. Development *134*, 4325–4334.

Gargano, J.W., Martin, I., Bhandari, P., and Grotewiel, M.S. (2005). Rapid iterative negative geotaxis (RING): a new method for assessing age-related locomotor decline in *Drosophila*. Exp. Gerontol. *40*, 386–395.

Geisbrecht, E.R., and Montell, D.J. (2004). A role for Drosophila IAP1-mediated caspase inhibition in Rac-dependent cell migration. Cell *118*, 111–125.

Gong, Q., Rangarajan, R., Seeger, M., and Gaul, U. (1999). The netrin receptor frazzled is required in the target for establishment of retinal projections in the Drosophila visual system. Development *126*, 1451–1456.

Harris, R., Sabatelli, L.M., and Seeger, M.A. (1996). Guidance cues at the *Drosophila* CNS midline: identification and characterization of two Drosophila Netrin/UNC-6 homologs. Neuron *17*, 217–228.

Hawkins, C.J., Yoo, S.J., Peterson, E.P., Wang, S.L., Vernooy, S.Y., and Hay, B.A. (2000). The Drosophila caspase DRONC cleaves following glutamate or aspartate and is regulated by DIAP1, HID, and GRIM. J. Biol. Chem. *275*, 27084–27093.

Hay, B.A., Wolff, T., and Rubin, G.M. (1994). Expression of baculovirus P35 prevents cell death in *Drosophila*. Development *120*, 2121–2129.

Hedgecock, E.M., Culotti, J.G., and Hall, D.H. (1990). The unc-5, unc-6, and unc-40 genes guide circumferential migrations of pioneer axons and mesodermal cells on the epidermis in C. elegans. Neuron *4*, 61–85.

Hidalgo, A., Kato, K., Sutcliffe, B., McIlroy, G., Bishop, S., and Alahmed, S. (2011). Trophic neuron-glia interactions and cell number adjustments in the fruit fly. Glia *59*, 1296–1303.

Higashijima, S., Shishido, E., Matsuzaki, M., and Saigo, K. (1996). eagle, a member of the steroid receptor gene superfamily, is expressed in a subset of neuroblasts and regulates the fate of their putative progeny in the Drosophila CNS. Development *122*, 527–536.

Jones, B.W., Fetter, R.D., Tear, G., and Goodman, C.S. (1995). glial cells missing: a genetic switch that controls glial versus neuronal fate. Cell *82*, 1013–1023.

Jordan, K.W., Carbone, M.A., Yamamoto, A., Morgan, T.J., and Mackay, T.F. (2007). Quantitative genomics of locomotor behavior in Drosophila melanogaster. Genome Biol. *8*, R172.

Kinrade, E.F., Brates, T., Tear, G., and Hidalgo, A. (2001). Roundabout signalling, cell contact and trophic support confine longitudinal glia and axons in the Drosophila CNS. Development *128*, 207–216.

Kolodziej, P.A., Timpe, L.C., Mitchell, K.J., Fried, S.R., Goodman, C.S., Jan, L.Y., and Jan, Y.N. (1996). frazzled encodes a *Drosophila* member of the DCC immunoglobulin subfamily and is required for CNS and motor axon guidance. Cell *87*, 197–204.

Kuo, C.T., Zhu, S., Younger, S., Jan, L.Y., and Jan, Y.N. (2006). Identification of E2/E3 ubiquitinating enzymes and caspase activity regulating Drosophila sensory neuron dendritic pruning. Neuron *51*, 283–290.

Kurada, P., and White, K. (1998). Ras promotes cell survival in Drosophila by downregulating hid expression. Cell *95*, 319–329.

Kuranaga, E., Kanuka, H., Tonoki, A., Takemoto, K., Tomioka, T., Kobayashi, M., Hayashi, S., and Miura, M. (2006). Drosophila IKK-related kinase regulates nonapoptotic function of caspases via degradation of IAPs. Cell *126*, 583–596.

Kuruvilla, R., Zweifel, L.S., Glebova, N.O., Lonze, B.E., Valdez, G., Ye, H., and Ginty, D.D. (2004). A neurotrophin signaling cascade coordinates sympathetic neuron development through differential control of TrkA trafficking and retrograde signaling. Cell *118*, 243–255.

Lai Wing Sun, K., Correia, J.P., and Kennedy, T.E. (2011). Netrins: versatile extracellular cues with diverse functions. Development *138*, 2153–2169.

Lanoue, B.R., and Jacobs, J.R. (1999). Rhomboid function in the midline of the *Drosophila* CNS. Dev. Genet. *25*, 321–330.

Li, J., Brieher, W.M., Scimone, M.L., Kang, S.J., Zhu, H., Yin, H., von Andrian, U.H., Mitchison, T., and Yuan, J. (2007). Caspase-11 regulates cell migration by promoting Aip1-Cofilin-mediated actin depolymerization. Nat. Cell Biol. *9*, 276–286.

Lowery, L.A., and Van Vactor, D. (2009). The trip of the tip: understanding the growth cone machinery. Nat. Rev. Mol. Cell Biol. *10*, 332–343.

McCall, K., Peterson, J.S., and Pritchett, T.L. (2009). Detection of cell death in *Drosophila*. Methods Mol. Biol. *559*, 343–356.

Mehlen, P., and Furne, C. (2005). Netrin-1: when a neuronal guidance cue turns out to be a regulator of tumorigenesis. Cell. Mol. Life Sci. *62*, 2599–2616.

Mehlen, P., Rabizadeh, S., Snipas, S.J., Assa-Munt, N., Salvesen, G.S., and Bredesen, D.E. (1998). The DCC gene product induces apoptosis by a mechanism requiring receptor proteolysis. Nature *395*, 801–804.

Meier, P., Silke, J., Leevers, S.J., and Evan, G.I. (2000). The Drosophila caspase DRONC is regulated by DIAP1. EMBO J. *19*, 598–611.

Mitchell, K.J., Doyle, J.L., Serafini, T., Kennedy, T.E., Tessier-Lavigne, M., Goodman, C.S., and Dickson, B.J. (1996). Genetic analysis of Netrin genes in *Drosophila*: Netrins guide CNS commissural axons and peripheral motor axons. Neuron *17*, 203–215.

Oppenheim, R.W., and von Bartheld, C. (2008). Programmed Cell Death and Neurotrophic Factors. In Fundamental Neuroscience, L.R. Squire, ed. (San Diego: Academic Press), pp. 437–468.

Oshima, K., Takeda, M., Kuranaga, E., Ueda, R., Aigaki, T., Miura, M., and Hayashi, S. (2006). IKK epsilon regulates F actin assembly and interacts with Drosophila IAP1 in cellular morphogenesis. Curr. Biol. *16*, 1531–1537.

Patel, N.H. (1994). Imaging neuronal subsets and other cell types in whole-mount Drosophila embryos and larvae using antibody probes. Methods Cell Biol. *44*, 445–487.

Pielage, J., Steffes, G., Lau, D.C., Parente, B.A., Crews, S.T., Strauss, R., and Klämbt, C. (2002). Novel behavioral and developmental defects associated with Drosophila single-minded. Dev. Biol. *249*, 283–299.

Rogulja-Ortmann, A., Lüer, K., Seibert, J., Rickert, C., and Technau, G.M. (2007). Programmed cell death in the embryonic central nervous system of Drosophila melanogaster. Development *134*, 105–116.

Rumpf, S., Lee, S.B., Jan, L.Y., and Jan, Y.N. (2011). Neuronal remodeling and apoptosis require VCP-dependent degradation of the apoptosis inhibitor DIAP1. Development *138*, 1153–1160.

Serafini, T., Kennedy, T.E., Galko, M.J., Mirzayan, C., Jessell, T.M., and Tessier-Lavigne, M. (1994). The netrins define a family of axon outgrowth-promoting proteins homologous to C. elegans UNC-6. Cell *78*, 409–424.

Sonnenfeld, M.J., and Jacobs, J.R. (1995). Apoptosis of the midline glia during Drosophila embryogenesis: a correlation with axon contact. Development *121*, 569–578.

Steller, H., Fischbach, K.F., and Rubin, G.M. (1987). Disconnected: a locus required for neuronal pathway formation in the visual system of Drosophila. Cell *50*, 1139–1153.

Tayler, T.D., Robichaux, M.B., and Garrity, P.A. (2004). Compartmentalization of visual centers in the Drosophila brain requires Slit and Robo proteins. Development *131*, 5935–5945.

Usui, N., Watanabe, K., Ono, K., Tomita, K., Tamamaki, N., Ikenaka, K., and Takebayashi, H. (2012). Role of motoneuron-derived neurotrophin 3 in survival and axonal projection of sensory neurons during neural circuit formation. Development *139*, 1125–1132.

Vanderhaeghen, P., and Cheng, H.-J. (2010). Guidance molecules in axon pruning and cell death. Cold Spring Harb. Perspect. Biol. *2*, a001859.

von Hilchen, C.M., Hein, I., Technau, G.M., and Altenhein, B. (2010). Netrins guide migration of distinct glial cells in the Drosophila embryo. Development *137*, 1251–1262.

Wang, H., and Tessier-Lavigne, M. (1999). En passant neurotrophic action of an intermediate axonal target in the developing mammalian CNS. Nature *401*, 765–769.

White, K., Grether, M.E., Abrams, J.M., Young, L., Farrell, K., and Steller, H. (1994). Genetic control of programmed cell death in Drosophila. Science *264*, 677–683.

Williams, D.W., Kondo, S., Krzyzanowska, A., Hiromi, Y., and Truman, J.W. (2006a). Local caspase activity directs engulfment of dendrites during pruning. Nat. Neurosci. *9*, 1234–1236.

Williams, M.E., Lu, X., McKenna, W.L., Washington, R., Boyette, A., Strickland, P., Dillon, A., Kaprielian, Z., Tessier-Lavigne, M., and Hinck, L. (2006b). UNC5A promotes neuronal apoptosis during spinal cord development independent of netrin-1. Nat. Neurosci. *9*, 996–998.

Xiong, W.C., and Montell, C. (1995). Defective glia induce neuronal apoptosis in the repo visual system of Drosophila. Neuron *14*, 581–590.

Yang, L., and Baker, N.E. (2003). Cell cycle withdrawal, progression, and cell survival regulation by EGFR and its effectors in the differentiating Drosophila eye. Dev. Cell *4*, 359–369.

Zhu, B., Pennack, J.A., McQuilton, P., Forero, M.G., Mizuguchi, K., Sutcliffe, B., Gu, C.J., Fenton, J.C., and Hidalgo, A. (2008). *Drosophila* neurotrophins reveal a common mechanism for nervous system formation. PLoS Biol. *6*, e284.